*Journal of Applied Electrochemistry* **32**: 259–265, 2002.



# The influence of electrode morphology on the performance of a DMFC anode

J. NORDLUND[1], A. ROESSLER[1,2] and G. LINDBERGH[1]
[1]*Department of Chemical Engineering and Technology, Applied Electrochemistry, KTH, SE-100 44 Stockholm, Sweden*
[2]*Present address: Laboratory of Chemical Engineering and Industrial Chemistry, Swiss Federal Institute of Technology, ETH, Zurich, Switzerland, CH-8093*

Received 25 July 2001; accepted in revised form 20 November 2001

*Key words:* direct methanol fuel cell anode, DMFC, gas evolution, mass transfer, PTFE

**Abstract**

For low concentrations of methanol, mass transfer in the electrode is a limiting parameter for the direct methanol fuel cell (DMFC). To improve mass transfer, it is possible to induce convection in the gas backing layer or even in the porous electrode. In this study electrodes with different amounts of PTFE were compared to observe the influence of morphology on the anode performance. The hypothesis was that adding PTFE to the anode may make the morphology more favourable for carbon dioxide to evolve as a gas by creating the necessary pore sizes. Electrode performance was characterized electrochemically and the anode layer structure was studied using SEM, Hg-porosimetry and the van der Pauw method for measuring electric conductivity. Pores smaller than 0.04 $\mu$m were unaffected by adding PTFE while the volume fraction of pores of 0.04–1.0 $\mu$m diameter increased. Electrodes with 50% PTFE also performed as nonhydrophobized, despite the much higher ohmic losses and thickness. This implies that, above a certain amount, adding PTFE has a positive effect and that optimizing the electrode with PTFE may give better performance than electrodes without PTFE. The results suggest that gas evolves within the electrode, giving improved mass transfer in the liquid phase.

## 1. Introduction

The direct methanol fuel cell (DMFC) is a promising power source for mobile, traction and smaller stationary applications. The DMFC has several advantages that suit these applications, including high efficiency, operating at, or near, ambient temperature, very low emissions, a potentially renewable fuel source, and fast and convenient refuelling.

DMFC uses methanol directly, in the form of vapour or liquid, to generate electrical energy. This makes the DMFC system much simpler than a fuel cell system in which hydrogen gas is produced by reforming of hydrocarbons. The anode reaction in the direct methanol fuel cell is given in Equation 1:

$$CH_3OH + H_2O \rightarrow 6\,e^- + 6\,H^+ + CO_2 \qquad (1)$$

The product, carbon dioxide, has limited solubility in the aqueous methanol solution and is therefore evolved as a gas in the cell at high current densities.

In a recent series of studies, a transparent acrylic DMFC, which made it possible to observe the gas evolution and two-phase flow in the anode flow channel, was used to study and improve the gas management [1–3]. Operation of the DMFC requires that the carbon dioxide gas and aqueous methanol solution move counter-currently in the catalyst layer and in the carbon cloth backing layer. A recent study shows that the mass transfer of methanol to the active layer of the anode limits the performance when concentration of methanol is lower than 1 M [4]. Therefore, there is a need to improve mass transfer from the fuel flow channel to the active sites in the electrode for low concentrations of methanol. There are three main ways to achieve improved mass transfer in the DMFC anode:
(i) Reducing the distance of diffusion/increasing the effective diffusion coefficient. This can be achieved by making the active layer and the gas backing layer thinner and/or making the respective layers more porous, thus increasing the effective diffusion coefficient.
(ii) Inducing convection from the fuel flow channel. A higher fuel flow velocity will give more convection induced into the gas-backing layer.
(iii) Inducing convection in/at the active layer. If gas is evolved in/at the active layer, convection will be induced, which could improve mass transfer.

A simple way to influence methanol mass transfer in the DMFC is to make the gas-backing layer hydrophobic. Argyropoulos *et al.* reported the influence of PTFE loading in the carbon cloth backing layer of a liquid-feed DMFC. At about 20% PTFE a maximum in cell

performance was found [5]. From these results it is interesting to see if the performance of the anode can be approved by adding PTFE to the active layer. To our knowledge no detailed study has yet been published about the influence of PTFE in the electrocatalytic layer on the performance of a liquid-feed DMFC. Therefore the aim of this work is to study the effect of adding PTFE into the catalytic layer. Electrochemical polarization curves combined with structure characterization and calculations of the critical radius of gas evolution are used to analyse the effect of different amounts of PTFE in the anode of the DMFC.

## 2. Theory of gas evolution

### 2.1. *Criteria for gas formation*

For a gas bubble to form and be stable in the porous electrode, the condition of nucleation has to be fulfilled and the radius of the bubble also has to be larger than the critical radius. Nucleation of a bubble can occur homogeneously or heterogeneously. Homogeneous nucleation implies that the bubble will form without the presence of a substrate. This typically requires high supersaturation and is not usually seen in porous structures [6–8]. Thus, heterogeneous nucleation is more probable for a porous electrode since irregularities where nucleation can occur are likely to be found.

The other criteria for gas formation is that the radius of the gas bubble has to be larger than the critical value where the force of surface tension of the liquid is balanced by the excess pressure within the gas bubble. This can be written in a general form where Henry's law is assumed to be valid:

$$xH - P_l \geq \frac{2\gamma}{W} \tag{2}$$

where the mole fraction, $x$, and the local pressure, $P_l$, are evaluated at the interface, $\gamma$ is the surface tension, $H$ is the Henry's law constant and $W$ is the characteristic length of the system, usually the radius at the smallest constriction in a converging–diverging geometry [7]. The supersaturation is given by $xH - P_l$.

### 2.2. *Gas evolution in the electrode: implications for mass transfer*

Mass transfer is enhanced by many different mechanisms when bubbles are formed in a system. The penetration effect, first described by Ibl [10] and since then continuously refined [11–15], is the convective mass transfer induced by a detached bubble to the spot from which it detached. The microconvective effect, described and modelled by Vogt et al. [16, 17], is the movement of the liquid pushed in the radial direction when a bubble grows. The macroconvective or the hydrodynamic effect is the mass transfer generated by the two-phase flow itself [10, 18–20]. At high production of carbon dioxide this effect will be considerable in the fuel channel since the gas flow will induce high linear velocities in the two-phase flow. The Marangoni effect is the mass transfer that originates from the surface tension gradient induced by the concentration gradient of carbon dioxide in the vicinity of the gas bubble [21].

## 3. Experimental details

For each of the different electrodes a separate ink was prepared. The components of the ink were 0.2 g supported catalyst, 2.667 g of 5 wt % Nafion dissolved in isobutanol, 0.25 g tetrabutylammonium hydroxide (TBAOH) and 3.55 g of isopropanol (IPA). The anode catalyst was PtRu (1:1) and cathode catalyst was Pt, both 40% wt % on Vulcan XC-72 (E-TEK). In subsequent steps each followed by mechanical stirring and immersion in an ultrasonic bath for more than 1 h, catalyst and Nafion were added followed by TBAOH/IPA. All PTFE-containing inks were prepared by mixing an already prepared catalyst ink with the desired amount of polytetrafluorethylene (PTFE) suspension (TF 5235 PTFE from Dyneon®), heavy shaking and ultrasonic treatment for more than 2 h. The PTFE suspension contained an emulsifier evaporating and/or decomposing below 150 °C.

MEAs with an active area of 1 $cm^2$, were manufactured by a spraying and hot-pressing method developed by Wilson and Gottesfeld [22, 23]. The corresponding ink was sprayed onto the cathode side of a dried and for 1 min hot-pressed (205 °C, 50 kg $cm^{-2}$) Nafion®-115-membrane, which had been previously cleaned and transformed into the $Na^+$ form by successively boiling in 3% $H_2O_2$ and 1 M NaOH for over 1 h in each step. Between each boiling procedure the membranes were washed in MilliQ water. After drying, the electrodes were hot-pressed at 205 °C, 50 kg $cm^{-2}$ for 1 min and the process was repeated on the other side of the membrane (usually the cathode side was the first one, to avoid changing the anode porosity by pressing the anode side twice). Finally, the Nafion® was reprotonated by boiling in 0.5 M sulfuric acid for more than one hour, followed by boiling in MilliQ water. The membranes were sandwiched between two E-TEK carbon cloth 'A' papers (10% PTFE content). All chemicals used were p.a. grade, Nafion® was supplied by DuPont and the TBAOH was 1.0 M in methanol supplied by Merck. This study covered a wide PTFE loading range from 0 to 50 wt % in electrodes with a constant PtRu (1:1) catalyst loading of $0.8 \pm 0.2$ mg $cm^{-2}$ and a constant Nafion® loading of 1.7 mg $cm^{-2}$.

The electrochemical characterization was performed in a cell with a geometric area of 1 $cm^2$, which was constructed in-house and is described in more detail elsewhere [24]. The current collectors were made of stainless steel with right-angled, spiral flow paths cut out for methanol and oxygen flow. 0.5 M Methanol (0.3 ml $min^{-1}$) was supplied to the anode by a peristaltic

pump (Watson Marlow) and preheated to the cell temperature (70 °C) before entering the cell. Oxygen (150 ml $min^{-1}$) was supplied to the cathode and humidified by MilliQ water at the cell temperature. To avoid measuring ohmic losses over the current collector–carbon cloth interface during the electrochemical measurements, two stainless steel wire probes were connected directly to the carbon cloth at the MEA. A dynamic hydrogen electrode (DHE) was used as reference. For the DHE to be stable over long periods of time, 80 $\mu$A was applied between the reference electrode and the cathode.

In this study the cell potential was swept slowly (typically 0.03 mV $s^{-1}$) from open circuit to zero cell potential and back to open circuit. The monitored hysteresis was small. Every curve was measured twice and averaged. All measurements were made with a potentiostat (PAR 263 A). An *x–t* recorder (BBC SE 120 Schreiber) recorded the potential of the anode against the reference electrode as the potentiostat controlled the cell voltage.

The electric conductivity in the lateral direction of the active layer was measured by the van der Pauw method [25]. All van der Pauw measurements were conducted at an air humidity of 33%, 23 °C (hygrometer: Vaisala HMI 41 indicator and HMP 42 prober). The measurements were made with an apparatus constructed in-house and a potentiostat (Solartron SI 1287, electrochemical interface) to set a current and to measure the potential difference. To obtain flat MEAs for the van der Pauw measurements the electrodes were hot-pressed (20 s, 100 °C, 50 kg $cm^{-2}$) as sample pretreatment.

The porous microstructure of the anode was studied with scanning electron microscopy (SEM) using a Jeol JSM-840 instrument. Samples of the MEA were cracked after cooling in liquid nitrogen and covered with a thin gold layer (~10 nm) by ion sputtering (Jeol Fine Coat Ion sputtering JFC-1100; 5 mA, 1200 V, 0.15 torr, 5 min).

The porosity and pore size distribution were obtained by Hg-porosimetry (Micromeretics pore sizer 9310). Values for the contact angle and the surface tension were assumed to be 130° and 485 mJ $m^{-2}$. To obtain reproducible values, electrodes with an area of 32 $cm^2$ were used.

## 4. Results

The influence of the PTFE content on the anode performance was analysed. The PTFE content in the anode catalyst layer was varied up to 60 wt %. At a content of 60 wt %, agglomerates of PTFE were visible as lumps. Therefore, only results for concentrations up to 50 wt % are considered in this study.

The nonhydrophobized MEAs gave the best performance of all electrodes (Figure 1). By increasing the PTFE content up to a value of about 10%, the anode performance deteriorated. At higher PTFE contents, performance improved and reached at 50 wt % PTFE, the same value as was observed with the electrodes without PTFE.

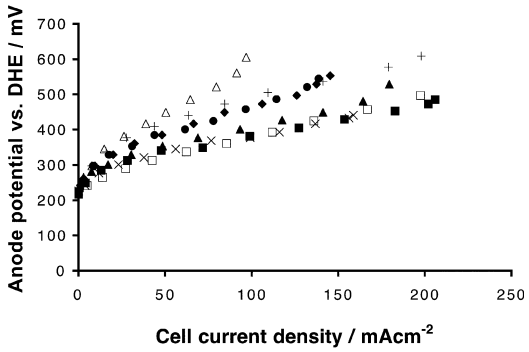


*Fig. 1.* Anode polarization curves for a DMFC (Nafion® 115, anode: 40 wt % Pt:Ru (1:1), cathode 40 wt % Pt, metal loading anode 0.8 mg $cm^{-2}$, Nafion® loading 1.7 mg $cm^{-2}$) at various PTFE contents in the anode catalyst layer; cathode 1 atm humidified $O_2$; anode 0.5 M methanol, 1 atm; 70 °C. Key: (■) 0, (▲) 2.5, (□) 5, (△) 10, (◆) 20, (●) 30, (+) 40 and (×) 50 wt % PTFE.

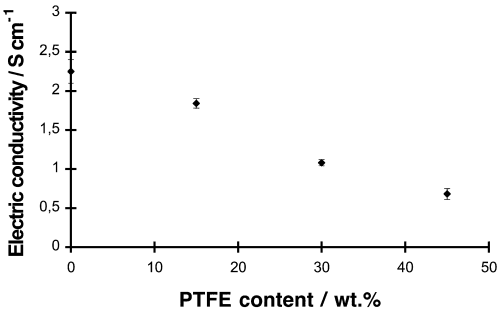


*Fig. 2.* Electronic conductivity in the anodic catalyst layer (Nafion® 115, anode Pt:Ru, metal loading 0.8 mg $cm^{-2}$, Nafion® loading 1.7 mg $cm^{-2}$) as a function of the PTFE content with error bars (confidence interval, 95%, $n = 4$). All measurements were conducted at an air humidity of 33%, 23 °C (hygrometer: Vaisala HMI 41 indicator and HMP 42 prober).

Figure 2 shows a summary of the values for the measured electric conductivity obtained in this work. They agree well with the values by Fischer et al. [26]. The clear trend that increasing the PTFE content decreases the electronic conductivity can be observed in Figure 2. It would also have been desirable to study the ionic resistance in the electrodes, but that was not possible within the scope of this paper.

Microstructure was studied using SEM. The presence of cracks increased in number and size with the PTFE loading. At a high PTFE content, PTFE fibres were seen in the electrode cross section (Figure 3). Such fibres were observed in other work, mostly when a rolling process was used [27, 28] but to our knowledge never when, as in this study, using a spraying technique. It is possible, however, that the fibres are an artefact due to the sample preparation.

Figure 4 shows the relation between the PTFE content and the thickness of the catalyst layer measured

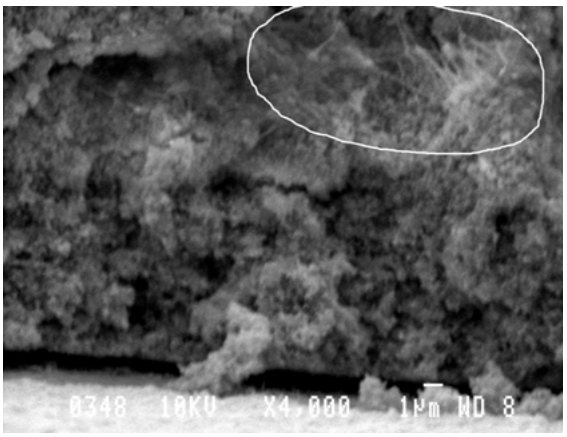


*Fig. 3.* SEM image of a cross-section of a MEA with 50 wt % PTFE content. Fibres are surrounded by a white circle.

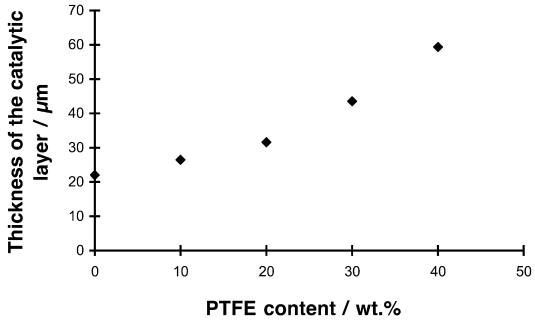


*Fig. 4.* Relation between the PTFE content of catalyst layer and thickness of catalyst layer.

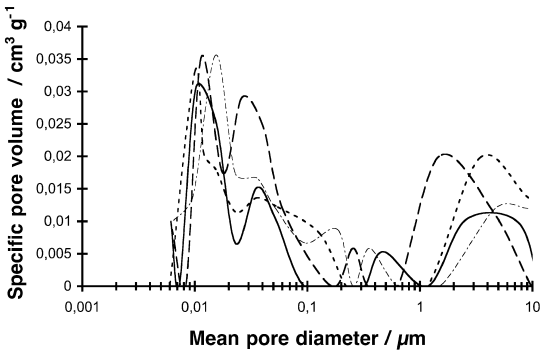


*Fig. 5.* Specific pore volume distribution in the MEAs of various PTFE contents with a Nafion® loading of 1.7 mg $cm^{-2}$ and a metal loading of 0.8 mg $cm^{-2}$ obtained by Hg-porosimetry. Key: (——) 0, (- - - -) 15, (– – –) 30 and (— —) 45% PTFE.

with SEM. It can be seen that the thickness increases with the PTFE content.

The specific pore volume distributions of the MEAs with various PTFE content are shown in Figure 5. The intrusion curves showed three pore zones with boundaries at approximately 0.04 and 1.0 $\mu$m. Pores between 0.01 and 0.04 $\mu$m are defined as primary pores and the ones between 0.04 and 1.0 $\mu$m are defined as secondary pores. It is obvious that the specific volume of secondary

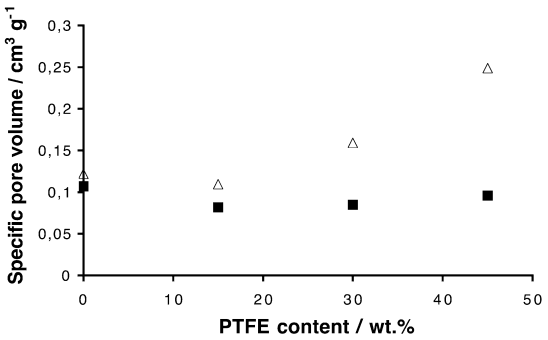


*Fig. 6.* Relation between specific pore volumes and PTFE content obtained by Hg-porosimetry. Key: (△) secondary pore (0.04–1.00 $\mu$m); (■) primary core (0.01–0.04 $\mu$m).

pores increases with the PTFE content. In contrast, PTFE has no influence on the primary pores. The relation between the pore volumes of primary and secondary pores and the PTFE content are shown in Figure 6. These results are in good agreement with other publications [29–31]. Small discrepancies are considered to result from differences in the preparation methods of the electrodes.

Watanabe et al. [29] identified the primary pores as the space between the primary particles in the agglomerate (carbon/Nafion®) and the secondary pores were those between the agglomerates. According to this theory, it can be emphasized that the PTFE exists only in the secondary pores, between agglomerates.

The content of PTFE influences the microstructure and the performance of the DMFC over the whole current density range, lowering performance. However, electrodes with 50 wt % PTFE have a performance similar to electrodes without PTFE, despite their thickness and a resistance that is eight times higher. Mass transfer has been shown to be very important in the anode of the DMFC [4] and the addition of PTFE seems to have a large influence on this.

To evaluate the critical radius for carbon dioxide bubbles in the electrode, Equation 2, the Henry constant and the surface tension of the fuel must be known. The values are derived from literature data as shown in Appendix A. The Henry constant, $H$, is $8.27 \times 10^5$ N $m^{-2}$ and the surface tension for 0.5 M methanol in water is $61.62 \times 10^{-3}$ N $m^{-1}$. The surface tension will change somewhat due to the surface activity of carbon dioxide as seen in Table 2, Appendix A. The surface tension can be approximated by the surface tension without carbon dioxide for low supersaturation of carbon dioxide. At high supersaturation, there is a notable decrease in surface tension.

Assuming gas evolution in the porous structure is not limited by nucleation, it is possible to calculate the supersaturation of carbon dioxide at which gas is formed for some different pore sizes. This can be achieved by evaluating Equation 2 for the conditions of the operating DMFC anode electrode. A typical primary pore size and two secondary pore sizes are

chosen: pores with a radius of 0.01 $\mu$m, a radius of 0.1 $\mu$m and a radius of 1 $\mu$m, where the latter two are the secondary pore sizes. Neglecting the influence of the surface activity of carbon dioxide, the necessary supersaturation to reach the critical radius is 123 bar, 12.3 bar and 1.23 bar, respectively.

At 1.23 bar supersaturation, the influence on surface tension of carbon dioxide is negligible. In the case of 0.1 $\mu$m radius, the 12.3 bar supersaturation of carbon dioxide will lower the surface tension. In Table 2, Appendix A, it is seen that at room temperature the surface tension is lowered by more than 20% at 12.3 bar supersaturation, giving a corrected value for the required supersaturation of about 10 bar. It is known, however, that the decrease in the surface tension is lower at higher temperatures, but there is still a considerable decrease in the surface tension [32]. For the 0.01 $\mu$m radius the value for surface tension is reduced even further, but the required supersaturation will still be very high [36]. An anode DMFC model assuming no gas evolution in the electrode shows that a supersaturation of 7 bar can be reached with a 23 $\mu$m thick electrode at high current densities [4]. A thicker electrode will give even larger supersaturation as a result of the increased distance for diffusion. The conclusion is that primary pores are too narrow for gas evolution, but gas will evolve at sufficient supersaturation in secondary pores.

## 5. Discussion

Figure 1 can be explained by combining characterization data with knowledge about mass transfer. There are positive and negative effects of the PTFE on the anode performance. Mass transfer limitation due to thicker electrodes with increasing PTFE content lowers anode performance. Adding PTFE also decreases the contact area between the polymer electrolyte and the catalyst clusters due to competition between the two polymers, that is, the utilization of the catalyst is lowered [22]. Another effect that lowers the performance is the higher electrical resistance when adding PTFE due to the lower electrical conductivity and the thicker electrodes as shown in Figures 2 and 4. It is most likely that the ionic resistance is increased in the same manner since the mechanism for lowering conductivity is the same. The negative effects combine to give lower performance with increasing PTFE content up to about 10 wt % of PTFE added. However, at PTFE contents higher than 10 wt %, the positive effects of PTFE addition begin to outweigh the negative effects, thus the improved performance.

Mass transfer, which is known to limit performance at low concentration of methanol [4], is thus improved by adding PTFE. From Figure 6 it can be seen that the secondary pore volume increases with an increasing amount of PTFE above 20 wt % of PTFE. This change in morphology provides room for the carbon dioxide to evolve as a gas, inducing convection in the electrode, thus improving mass transfer within the electrode. It is possible that continuous channels of hydrophobous PTFE are formed at high PTFE concentrations making it possible for gaseous carbon dioxide to leave the anode. Carbon dioxide at neighbouring hydrophilic areas will provide the channel with carbon dioxide by diffusion and induced convection as discussed by Chirkov and Pshenichnikov [33]. The improved morphology for gas evolution by increased pore sizes is perhaps not the only positive influence of the added PTFE. The PTFE also influences the contact angle and the ratio of hydrophobic/hydrophilic areas.

Since Nafion® loading was kept constant in this study, the electrodes were far from optimized, especially at higher PTFE contents. It is most probable that optimizing Nafion® content in these electrodes would lead to better performing electrodes. It would be even better to optimize the ratio: PTFE:Nafion®:PtRu/C. However, the method of preparation may strongly influence the results from adding PTFE to the electrode. There are many different methods to introduce PTFE into the catalyst layer and sometimes there are combinations of techniques (e.g., a small amount is mixed with carbon powder in dry conditions and afterwards PTFE in suspension is added [34]).

## 6. Conclusions

The effect of adding PTFE to the microstructure in the catalyst layer was investigated. Although with up to 10 wt % PTFE added to the electrode the performance was lowered, above 10 wt % PTFE there was a gradual increase in performance. At 50 wt % PTFE the performance was similar to electrodes with no added PTFE, despite the fact that the electrodes with 50 wt % PTFE are much thicker, potentially have a much larger mass transfer resistance, an eight times higher electric resistance and most likely a much lower ionic conductivity. This implies that, above a certain amount, adding PTFE has a positive effect that outweighs the negative effects, as a result, optimizing the electrode with PTFE may give better performance than electrodes without PTFE. Mercury porosimetry shows that the electrodes have two distinctive pore distributions with a boundary at about 0.04 $\mu$m where only the larger distribution (secondary pores) is affected by adding PTFE. The amount of secondary pores increases with increasing PTFE content starting at about 20 wt % PTFE. Electric conductivity decreases with increasing PTFE content. Cracks in the catalyst layer increase in number and size with higher PTFE content. The critical radius of carbon dioxide gas is within the scope of the secondary pores; thus gas formation within the porous electrode is possible.

## Acknowledgements

The authors acknowledge Dr Anders Lundblad, KTH, for his valuable help and support when dealing with the

non-electrochemical characterisation techniques and Dr Philip Byrne, Comsol AB, for gas evolution literature and valuable discussions. The financial support of Volvo Technical Development and the Swedish National Energy Administration is gratefully acknowledged. J. Nordlund also gratefully acknowledges a scholarship from the Ernst Johnson Foundation.

## References

1. P. Argyropoulos, K. Scott and W.M. Taama, *J. Appl. Electrochem.* **29** (1999) 661.
2. K. Sundmacher and K. Scott, *Chem. Eng. Sci.* **54** (1999) 2927.
3. P. Argyropoulos, K. Scott and W.M. Taama, *Electrochim. Acta* **44** (1999) 3575.
4. J. Nordlund and G. Lindbergh, submitted to *J. Electrochem. Soc.*
5. K. Scott, W.M. Taama and P. Argyropoulos, *J. Appl. Electrochem.* **28** (1998) 1389.
6. J. Kamath and R.E. Boyer, 68th Annual Technical Conference and Exhibition of the SPE, Houston, TX, 3–6 Oct. 1993.
7. Y.C. Yortos and M. Parlar, 64th Annual Technical Conference and Exhibition of the SPE, San Antonio, TX, 8–11 Oct. 1990.
8. R.B. Dean, *J. Appl. Phys.* **15** (1944) 446.
9. P.M. Wilt, *J. Colloid Interface Sci.* **112** (1986) 530.
10. N. Ibl, E. Adam, J. Venczel and E. Schalch, *Chem. Ing. Tech.* **43** (1971) 202.
11. J. Venczel, Über den Stofftransport an gasentwickelnden Elektroden, *Diss. ETH*, Zürich (1961).
12. N. Ibl and J. Venczel, *Metalloberfläche* **24** (1970) 365.
13. N. Ibl, *Chem. Ing. Tech.* **35** (1963) 353.
14. I. Rousar and V. Cezner, *Electrochim. Acta* **20** (1975) 289.
15. L.J.J. Janssen and S.J.D. van Stralen, *Electrochim. Acta* **26** (1981) 1011.
16. H. Vogt, Ein Beitrag zum Stoffübergang an gasentwickelnden Elektroden, Diss. University of Stuttgart (1977).
17. K. Stephan and H. Vogt, *Electrochim. Acta* **24** (1979) 11.
18. L.J.J. Janssen and J.G. Hoogland, *Electrochim. Acta* **18** (1973) 543.
19. L.J.J. Janssen and J.G. Hoogland, *Electrochim. Acta* **15** (1970) 1013.
20. L.J.J. Janssen and E. Barendrecht, *Electrochim. Acta* **24** (1979) 693.
21. N.G. McDuffie, *Chem. Eng. Sci.* **54** (1999) 1155.
22. M.S. Wilson and S. Gottesfeld, *J. Appl. Electrochem.* **32** (1992) 1.
23. M.S. Wilson, J.A. Valerio and S. Gottesfeld, *Electrochim. Acta* **40** (1995) 355.
24. J. Ihonen, F. Jaouen, G. Lindbergh and G. Sundholm, *Electrochim. Acta* **46** (2001) 2899.
25. L.J. van der Pauw, *Philips Res. Reports* **13** (1958) 1.
26. A. Fischer, J. Jindera and H. Wendt, *J. Appl. Electrochem.* **28** (1998) 277.
27. M. Schulze, M. von Bradke, R. Reissner, M. Lorenz and E. Gülzow, *Fresen. J. Anal. Chem.* **365** (1999) 123.
28. R. Holze and A. Maas, *J. Appl. Electrochem.* **13** (1983) 549.
29. M. Watanabe, M. Tomikawa and S. Motoo, *J. Electroanal. Chem.* **195** (1985) 81.
30. M. Watanabe, K. Makita, H. Usami and S. Motoo, *J. Electroanal. Chem.* **197** (1986) 195.
31. M. Uchida, Y. Aoyama, N. Eda and A. Ohta, *J. Electrochem. Soc.* **142** (1995) 4143.
32. C. Jho, D. Nealon, S. Shogbola and A.D. King Jr, *J. Colloid Interface Sci.* **65** (1978) 141.
33. Y.G. Chirkov and A.G. Pshenichnikov, *Soviet Electrochem.* **26** (1990) 1379.
34. Y. Kiros and S. Schwartz, *J. Power Sources* **87** (2000) 101.
35. Solubility data series, Vol. 62, IUPAC, Oxford, GB (1996).
36. Landolt–Börnstein, New Series IV/16, p. 311, Springer, Germany (1997).
37. Landolt–Börnstein, New Series IV/16, p. 18, Springer, Germany (1997).
38. Landolt–Börnstein, New Series IV/16, p. 52, Springer, Germany (1997).
39. R.H. Perry, D.W. Green, 'Perry's Chemical Engineers Handbook' 7th edn., p. 2–373.
40. S.D. Lubetkin and M. Akhtar, *J. Colloid Interface Sci.* **180** (1996) 43.

## Appendix A

The Henry constant, $H$, is taken as

$$\ln(H) = 4.800 + 3934.3 \times T^{-1} - 941290.2 \times T^{-2} \quad (3)$$

where $H$ is given in bar and the temperature, $T$ in kelvin [35]. Equation 3 is valid for $T$ between 273 and 353 K and the standard deviation in the fitted data is 1.1% in $H$. The equation is derived for carbon dioxide over pure water. In this paper it is assumed that adding small amounts of methanol will not change the Henry constant. The surface tension is a function not only of temperature, but also of partial pressure of carbon dioxide and of concentration of methanol in the fuel. The surface tension of a methanol–water mixture is given in Landolt–Bernstein [36] but only at 20 °C. The surface tension of the pure liquids is given as function of

*Table 1.* Surface tension at 343 K for a mixture of water and methanol at different concentrations

| $C_{MeOH}$ /mol dm$^{-3}$ | Surface tension /mN m$^{-1}$ |
|---|---|
| 0.001 | 64.46 |
| 0.003 | 64.45 |
| 0.005 | 64.44 |
| 0.01 | 64.41 |
| 0.3 | 62.74 |
| 0.5 | 61.62 |
| 1 | 58.93 |
| 3 | 49.51 |
| 5 | 41.89 |

*Table 2.* Surface tension of water as a function of partial pressure of carbon dioxide at 21 °C

| Partial pressure of carbon dioxide/bar | Surface tension /mN m$^{-1}$ |
|---|---|
| 0 | 72.6 [37] |
| 1 | 70.4 |
| 2 | 67.3 |
| 3 | 64.3 |
| 4 | 62.4 |
| 5 | 61.2 |
| 6 | 60.1 |
| 7 | 59.3 |
| 8 | 58.3 |
| 9 | 57.9 |
| 10 | 56.7 |

temperature in Landolt–Bernstein [37, 38]. The surface tension of the mixture at elevated temperatures can be calculated using the formula

$$\sigma_{\text{mixture}}^{1/4} = \psi_{\text{w}}\sigma_{\text{w}}^{1/4}\psi_{\text{org}}\sigma_{\text{org}}^{1/4} \tag{4}$$

where $\psi_{\text{org}} = 1 - \psi_{\text{w}}$ and $\psi_{\text{w}}$ are a complex functions of the mole fractions, the molar volumes of the components, the temperature and a factor depending on size and type of organic component [39]. The resulting surface tension at 343 K is presented in Table 1.

Ludbetkin and Akhtar [40] investigated the influence of the partial pressure of carbon dioxide on the surface of water and found that surface tension decreases with increasing pressure of carbon dioxide at 21°C. The results of their measurements are given in Table 2.